MitoFit Preprints 2023.4
https://doi.org/10.26124/mitofit:2023-0004

Technical Communication

Cite
Rodríguez E, Bettinazzi S, Inwongwan S, Camus MF, Lane N (2023) Harmonising protocols to measure *Drosophila* respiratory function in mitochondrial preparations. MitoFit Preprints 2023.4. https://doi.org/10.26124/mitofit:2023-0004

Author contributions
ER, SB, SI: study design, experimental work and manuscript preparation. FC: experimental work and manuscript preparation; NL: manuscript preparation and funding.

Conflicts of interest
The authors declare no conflicts of interest

Online 2023-04-05

Data availability
Original files will be available Open Access (in preparation)

Keywords
Drosophila; mitochondria; respirometry; oxygen diffusion; fluorescence; reproducibility

Harmonising protocols to measure *Drosophila* respiratory function in mitochondrial preparations

Enrique Rodríguez[1*], Stefano Bettinazzi[1], Sahutchai Inwongwan[1,2], M. Florencia Camus[1], Nick Lane[1]

[1] Research Department of Genetics, Evolution and Environment, University College London, UK
[2] Department of Biology, Faculty of Science, Chiang Mai University, Thailand

* Corresponding author: enrique.rodriguez@ucl.ac.uk

Summary

Recent advances in fluorespirometry have allowed to measure multiple parameters of mitochondrial function; yet protocols vary widely between research groups, organisms, and tissues, sometimes without adequate justification or with assumptions that are not supported by data. This is particularly clear in *Drosophila* studies, a common model organism in biological research, with increasingly popularity in mitochondrial research. We first surveyed the literature on *Drosophila* fluorespirometry to compare and contrast approaches used in the field. Then, we showed that contrary to previous assumptions based on mammalian studies, oxygen diffusion is not limited in the permeabilised thoracic muscle of this species. We further compared the permeabilization and homogenising approaches, showing the former to be more adequate in *Drosophila*. Finally, we assessed the concentration-dependent effect of various commonly used fluorescent probes on mitochondrial respiration, showing that some probes strongly affect mitochondria and that careful choice of concentration and probe needs to be taken. The objective of this study is to give recommendations and work towards a harmonisation of the protocols for assessing mitochondrial function in fruit flies.

1. Intorduction

Drosophila species, and in particular *D. melanogaster,* are widely recognised and used as powerful model organisms in biological and biomedical research (Markow, 2015). In the last decade, *Drosophilae* have been increasingly used to investigate the roles of mitochondria in diseases, environmental change, and evolutionary biology (Camus et al., 2012, Carnegie et al., 2021, Cormier et al., 2019, Jørgensen et al., 2021, Pichaud et al., 2011, Rodríguez et al., 2021, Wolff et al., 2016). Since the development and increase in popularity of high-resolution fluorespirometry to analyse mitochondrial function, researchers have often sought to adapt existing protocols (often developed on murine and human models) to measure *Drosophila* mitochondrial respiration. A survey of the literature quickly shows the wide variety of methods for studying *Drosophila* using the O2k FluoRespirometer (Oroboros Instruments, Innsbruck, Austria), but the choice of these protocols often lacks clear justification, reasoning or adaptation to the fruit flies' fundamentally different biology. This makes it challenging for researchers new to fluorespirometry to choose the optimal sample preparation or analytical protocol for their specific questions, undermining efforts to improve reproducibility and confidence in cross-study comparisons in the field (Baker, 2016). The precision and accuracy of fluorespirometry strongly depend on sample preparation, as well as instrument parameters and choice of substrate-uncoupler-inhibitor-titration protocol (SUIT, Gnaiger 2020). Different types of mitochondrial (mt) preparations are available to address specific study questions (Doerrier et al., 2018). These are commonly: isolated mitochondria (imt), tissue homogenate (thom), permeabilized muscle fibres (pfi), and permeabilized cells (pce). These preparations differ in whether the organelle is selectively removed from the cellular environment (imt), or whether mechanical (thom) and/or chemical permeabilization is performed (pfi, pce) with the cytosol washed out (Kuznetsov et al., 2008, Pesta and Gnaiger, 2015), to allow the exchange of soluble molecules across the plasma membrane without damaging the mitochondrial membranes (Gnaiger et al., 2020). The choice of mitochondrial preparation comes with advantages and pitfalls which have been raised and discussed in the past for other animal models; however, *Drosophila* have so far escaped careful scrutiny.

The first problematic issue concerns the optimal oxygen saturation for measuring mitochondrial bioenergetics in the different sample preparations. This is particularly pressing when using permeabilized tissues rather than isolated mitochondria. For instance, while many studies using *Drosophila* thorax pfi advocate the oversaturation of oxygen concentrations in the respiration chambers, others simply work at ambient oxygen levels (Correa et al., 2012). Addition of exogenous oxygen is argued to overcome the potential diffusion limit of oxygen across the fibres and avoid measuring mitochondria in hypoxic or anoxic states. In a mammalian study by Pesta and Gnaiger (2012), the apparent K_m for oxygen, or c_{50}, was found to be around 40–50 µM in rat and human permeabilized tissues (soleus, heart, vastus lateralis), 100-fold above that of isolated mitochondria in ADP-stimulated respiration. The oxygen-dependence analyses of these tissues show a near hyperbolic behaviour of O_2 flux, which is improved with mechanical disturbance of the fibres (*ibid*). The authors concluded that elevating oxygen concentration in the chamber was necessary in pfi to avoid hypoxic or anoxic cores in the fibre bundles, not due to the kinetics of mitochondria, but rather to the diffusion distances being much greater in these fibre bundles than in pce or imt. They recommended that chamber oxygen levels should be kept in the range of 250–500 µM when using pfi. In flies,

the thoracic flight muscle tissue is assumed to exhibit equivalent limitations in oxygen delivery (Correa et al., 2012), but this was based on mammalian studies. Oxygen delivery in the insect flight muscle is critical given the high metabolic activity needed to support flight: they sustain the highest mass-specific metabolic rate of any animal, thanks in part to densely-packed mitochondria (Suarez, 2000, Suarez, 1998). However, to our knowledge, no study has assessed whether this limit does indeed exist. The fact that oxygen delivery to fly muscle tissue is done via tracheoles rather than capillaries might be beneficial, even more so in the context of permeabilised tissue in a respirometry chamber. Importantly, increasing O_2 concentration in the media also has potential downsides. In particular, the H_2O_2 signal depends on both the buffer and the O_2 concentration (Puma et al., 2020). Given that a higher O_2 concentration in the chamber increases H_2O_2 flux, pfi (associated with hyperoxic conditions) is often considered to be unsuitable for the measurement of H_2O_2 flux (Oroboros-Ecosystem, 2016). Experimenters have therefore generally used imt rather than pfi for fluorespirometry to overcome this limitation. Overall, establishing a reliable and shared protocol that may circumvent the hyperoxygenation issue is now an urgent priority for fluorespirometry.

This concern leads us to the second critical issue, relating to the overall reliability of the various mitochondrial preparations. Among the three major techniques (i.e. thom, pfi, imt), isolated mitochondria and permeabilized fibres are those most commonly adopted in the respirometry field (see Table 1). Using imt has potential disadvantages, as removing the organelle from its general cellular context risks stripping away critical mediators or membrane synapses that maintain mitochondrial function when working at the level of whole tissue, so long as oxygen delivery is appropriate. Tissue homogenates have also been increasingly used as a valid alternative to pfi and isolated mitochondria to study bioenergetics in a variety of tissues and species (Pecinová et al., 2011, Quéméneur et al., 2022, Thoral et al., 2021). The advantages of this technique include fast preparation following dissection of the tissue of interest, lower perturbation of the "native" cellular environment (as opposed to imt), as well as easy access to excess sample to normalise the results by protein content or another marker of mitochondrial content (such as citrate synthase activity or mtDNA copy number), without relying on the leftover tissue retrieved from the chamber itself, which might not be accurate. Despite the potential benefits that the thom technique might have, no study has assessed the suitability of thom preparations obtained with *Drosophila* thoraces and compared their quality with more conventional pfi and imt approaches. Confidence in this preparation technique is of great importance, especially for experimental designs that are high-volume, time-consuming and costly to run.

A third important point concerns the fluorescent probes and their impact on mitochondrial respiration. The recent development of fluorescent probes for high-resolution fluorespirometry allows the combination of oxygen flux measurement with other relevant mitochondrial parameters, including H_2O_2 flux, membrane potential, rates of ATP production, and calcium flux. Nonetheless, papers using these methods on *Drosophila* flies are scarce and seldom mention method development regarding the issue of whether the probes themselves affect mitochondrial function (and if so, to what extent). Therefore, it is vital to appreciate the right chemicals and concentration for comparative and reproducibility purposes. One critical, frequently overlooked factor in mitochondrial studies is the difference in respiration or response to treatments between males and females, of concern since males remain overrepresented in animal studies (Zucker and Beery, 2010). For example, our own earlier work (Camus et al., 2022) has shown that

female flies are more reliant on Complex I, which makes them especially vulnerable to its suppression, potentially by fluorespirometric probes, which could impact measurements of membrane potential, ROS flux and ATP synthesis. This is not least concerning in the face of growing evidence pointing toward sex-specific diseases and dysfunctions (Morrow, 2015, Ventura-Clapier et al., 2017). It is clearly important to optimise protocols for both male and female tissue function, and to fully anticipate where differences might lie, or where the methodology used might obfuscate the results.

The aim of this study was to address all these questions in *Drosophila*, to give researchers better confidence in the analysis and quality of their data. First, we surveyed the O2k literature on *Drosophila* to get a sense of distribution of strains, sex, and methods used by laboratories across the world, which are reported in Table 1. We then experimentally compared rates of O_2 flux in permeabilized fibres of *Drosophila* males and females with and without oversaturation with added O_2 in the chamber, as well as with isolated thorax mitochondria, to assess whether there exists a limit to oxygen diffusion in this model. Subsequently, we compared mitochondrial preparations of pfi to thom at the levels of O_2 and H_2O_2 flux, and we finished by evaluating the effect of commonly used fluorescent probes on *Drosophila* O_2 flux.

2. Materials and methods

2.1. Literature survey of *Drosophila* studies in the O2k Respirometer

We explored the methodological sections of all the O2k-network publications stored on the "mitopedia" (Oroboros-Ecosystem, 2023) up to 01-06-2022, as well as through a Google Scholar search of "*Drosophila*" AND "Oroboros". For each study, we report the *Drosophila* species and strains used, the sex and life stage, tissue, mitochondrial preparation, respiration buffer, O2k temperature, whether additional oxygen was added to the chambers, if ROS was measured simultaneously, and the reported *RCR*s of the youngest or control flies studied (Table 1).

2.2. Fly maintenance

All *D. melanogaster* were maintained on a standard mix of molasses/cornmeal medium at a constant 25 °C on a 12/12 hour light/dark cycle, RH=50 %. 2–5 days old male and female flies from the wild type (WT) strain were used, where the $w^{1118\text{-}5095}$ nuclear genome is coevolved with the mitochondrial genome (Rodríguez et al., 2021).

2.3. Preparation of fly permeabilized thoraces

Preparation of *Drosophila* permeabilized fibres (pfi) was based on a slightly modified version of Simard et al. (2018). Male or female WT flies were dissected on ice in groups of three. First, head, abdomen, wings and legs were removed, and three thoraces were put in 1 mL ice-cold preservation solution (BIOPS; 2.77 mM CaK_2EGTA, 7.23 mM K_2EGTA, 5.77 mM Na_2ATP, 6.56 mM $MgCl_2$, 20 mM taurine, 15 mM Na_2phosphocreatine, 20 mM imidazole, 0.5 mM dithiothreitol, and 50 mM K-MES, pH 7.1) in a 24-well plate. Then, 80 $\mu g \cdot mL^{-1}$ saponin (5 $mg \cdot mL^{-1}$ stock solution in BIOPS) was added, shaken for 20 min on an orbital shaker, and rinsed with shaking for 5 mins in respiration buffer MiR05 (0.5 mM EGTA, 3 mM $MgCl_2 \cdot 6H_2O$, 60 mM lactobionic acid, 20 mM taurine, 10 mM KH_2PO_4, 20 mM HEPES, 110 mM D-sucrose, 1 g/L bovine serum albumin, pH 7.1). The

thoraces were then carefully dry-weighed and transferred to each O2k-chamber, prefilled with 2.1 mL MiR05 respiratory buffer and kept at 25 °C. Experiments ran as explained in the corresponding sections below.

2.4. Mitochondrial isolation of fly thoraces

A total of 30 male or female of our WT strain were dissected on ice with a few drops of mitochondrial isolation buffer (250 mM sucrose, 5 mM trizma base, 2 mM EGTA, 1 % w/v bovine serum albumin, pH 7.4). Head, abdomen, wings and legs were removed and only thoraces were kept, then transferred to an Eppendorf 1.5 mL tube containing 200 µL of buffer. Thoraces were homogenised with a handheld homogenizer with a blue polypropylene pestle (100 back-and-forth passes), then filtered in a 1 mL syringe containing a small piece of gauze and transferred to another Eppendorf, with an additional 625 µL of mitochondrial isolation buffer. The homogenate was then centrifuged at 300 *g*, 4 °C for 3 minutes, filtered on gauze to a new tube as previously described, and centrifuged at 9000 *g*, 4 °C for 10 minutes. The supernatant was discarded, and the mitochondrial pellet was rinsed twice in 150 µL of isolation buffer, and finally resuspended in 60 µL of the same buffer. Protein content was then determined using the QuantiPro BCA assay kit (Sigma-Aldrich QPBCA-1KT), and mitochondrial isolate was added to a final concentration of 0.05 $mg \cdot mL^{-1}$ in the chamber.

2.5. Oxygen diffusion limit

The oxygen dependence of respiration of permeabilized fibres (pfi) of fly thoraces in hyperoxic (n=13) or normoxic (n=6) conditions was investigated following the trend of O_2 flux (oxygen consumption) at decreasing O_2 concentration. We used an Oxygraph-2K (Oroboros Instruments, Innsbruck, Austria) and followed the protocol established by Pesta and Gnaiger (2012). Specifically, N-pathway substrates pyruvate (P, 10 mM) and malate (M, 2 mM) were added to the chamber containing the permeabilized thoraces at air saturation. For hyperoxic conditions, pure oxygen was added up to a concentration range of 400–500 µM. Chambers were closed and LEAK-state respiration was allowed to stabilise for about 15 min, after which ADP (D, 5 mM) was added to reach phosphorylating N-linked respiration. Cytochrome *c* was added (c, 10 µM) to assess the integrity of the outer mitochondrial membrane. Runs where respiration increased over 15 % were discarded. Then, proline (Pro, 10 mM) and succinate (S, 10 mM) were added to reach maximum coupled N and S-pathway respiration, and oxygen was allowed to be consumed. During that time, O_2 flux and its linked O_2 concentration were measured at different time points, up until complete depletion of oxygen in the chambers. Then, they were reoxygenated by opening of the chambers until saturation, closing and the O_2 flux was allowed to stabilise again. Air oxygen calibrations were performed daily, and instrumental and zero oxygen calibrations were performed at every change of MiR05 stock. All data were normalised for an internal parameter, i.e. the maximal coupled respiration achieved during the run, and expressed as flux control ratios (*FCR*, see Gnaiger et al., 2020). For each run, *FCR*s were plotted as a function of oxygen concentration (Figure 2A). The best-fit curved logarithmic trendline was calculated and its equation used to extrapolate the apparent K_m for oxygen, or c_{50}, i.e. the O_2 concentration (µM) at which O_2 flux halves (*FCR* = 0.5, Figure 2B, Table S1).

2.6. Comparison of thorax permeabilized fibres and homogenates

We compared the standard thorax pfi preparation protocol (see "Preparation of fly permeabilized thoraces" section above) to various preparations of thom in WT females, using a specially designed tissue shredder (PBI-Shredder SG3, Pressure Biosciences, Medford, MA, USA) or a standard pellet pestle hand-held tissue homogenizer (Kimble Kontes Pellet Pestle Cordless Motor, DWK Life Sciences, Mainz, Germany). We followed the SUIT protocol detailed in Rodríguez et al. (2021). First, measurement of H_2O_2 was possible due to the initial addition of 15 µM DTPA, 5 U/mL SOD, 1-unit HRP, and 10 µM Amplex Ultra Red to the chamber. NADH-pathway substrates pyruvate (10 mM) and malate (2 mM) were added, followed by the pfi. Chambers were closed, after which N-LEAK state (N_L) respiration was allowed to stabilize for 15 min, then ADP (5 mM) was injected to stimulate N-OXPHOS respiration (N_P), followed by proline (10 mM, $NPro_P$), succinate (10 mM, $NProS_P$), and glycerol phosphate (10 mM, $NProSGp_P$) at the end of which the maximum coupled respiration rate was reached. The uncoupler FCCP was added in 0.5 µM steps to measure maximum uncoupled respiration ($NProSGp_E$). Then, inhibitors were added: rotenone inhibiting the N-pathway (0.5 µM, $ProSGp_E$), malonate to block the S-pathway (5 mM, $ProGp_E$), and finally inhibition of Complex III was achieved with antimycin A (2.5 µM), which also allowed the estimation of residual oxygen consumption (ROX). The OXPHOS coupling efficiency (j≈*P*) with N-pathway substrates was calculated as: $1-(N_L/N_P)$.

2.7. Effect of fluorescent probes on respiration

All fluorophores were prepared according to the protocols published on the MitoPedia (Oroboros Instruments, Innsbruck, Austria). WT female *Drosophila* thorax pfi were prepared as described in the section above, and were added to the chamber containing pyruvate (P, 10 mM) and malate (M, 2 mM). After addition of ADP (D, 5 mM) and cytochrome *c* (c, 10 µM), each fluorophore was titrated into the O2k chamber with stepwise increases in concentrations (specified in the following sections). In a parallel chamber, stepwise additions of the solvent without the fluorophore (DMSO, H_2O or ethanol) were done simultaneously.

Amplex Ultra Red: The H_2O_2 detection probe Amplex Ultra Red (AmR, Thermo Fisher A36006) was prepared at a stock solution concentration of 10 mM in fresh DMSO (https://wiki.oroboros.at/index.php/Amplex_UltraRed), and tested at concentrations ranging from 2.5 to 15 µM (a series of six 0.5 µL injections).

Magnesium Green: The probe used to measure ATP production rates, Magnesium Green (MgG, Thermo Fisher M3733), was prepared at a concentration of 1.1 mM in H_2O (https://wiki.oroboros.at/index.php/Magnesium_Green), and tested at concentrations ranging from 0.275–1.65 µM (six 0.5 µL injections).

Rhodamine 123: A 0.2 mM stock solution of membrane potential probe rhodamine 123 (Rh123, Thermo Fisher R302) was prepared in ethanol (https://wiki.oroboros.at/index.php/Rhodamine_123), and tested at concentrations ranging from 0.2 to 1.2 µM (six 2 µl injections).

Safranin: A 1 mM stock solution of membrane potential probe Safranin (Saf, Sigma S2255) was prepared in H_2O as instructed (https://wiki.oroboros.at/index.php/Safranin), and titrated at 0.5 µM increments, until a final concentration of 3.0 µM (six 1 µl injections).

TMRM: A 1 mM stock solution of membrane potential probe Tetramethyrhodamine methyl ester perchlorite (TMRM, Sigma T5428) was prepared in fresh DMSO (https://wiki.oroboros.at/index.php/TMRM), and 0.5 µM titration steps were added to the chamber until a final concentration of 3.0 µM (six 1 µl injections).

Respirometry data were normalised for a common internal parameter, the CI-sustained coupled respiration in absence of fluorescent probes (N_{CP}), and expressed as flux control ratios (*FCR*). Parallel controls were titrated with an equal volume of each probe-specific solvent.

2.8. Data analysis

O2k fluorespirometry data were extracted using DatLab 7.4 software (Oroboros Instruments, Innsbruck, Austria). For the oxygen diffusion limit experiment, the comparison of c_{50} values between pfi in normoxic or hyperoxic conditions was carried out by means of a two-samples Student's *t* test. Data are presented in Table S1 as mean ± standard error of the mean (s.e.m). Differences in oxygen and hydrogen peroxide fluxes, dictated by the different method for sample preparation (pfi or thom) were determined through two-samples Student's *t* tests, for each parameter separately. The effect of fluorescent probe presence was inferred at each titration point by means of a two-samples *t* test. *P*-values were adjusted using Holm's correction for multiple testing. The normality and homogeneity of variance were verified with Shapiro and Levene's tests respectively. Graphics and statistical analyses were performed using MS Excel (Microsoft Corporation, 2021) and R ggplot2 package (R Team, 2016) software. Summaries are provided in Tables S1 and S2.

3. Results

3.1. A variety of approaches to assess mitochondrial function in *Drosophila*

Table 1 shows the different approaches to studying *Drosophila* mitochondrial bioenergetics in a total of 60 studies found over the last 12 years. *Drosophila melanogaster* was the preferred species in 56 out of 60 studies, with a wide variety of strains; 3 studies used *D. simulans* (Pichaud et al., 2012, Pichaud et al., 2011, Pichaud et al., 2010), while 1 study compared six different *Drosophila* species, among which *melanogaster* (Jørgensen et al., 2021). Adult flies were used in 50 papers. Males were overly represented with 25 studies, while females were found in 10 studies. Both sexes were compared in only 9 reports, while 7 did not specify the sex. Moreover, 11 papers reported using larvae but failed to report the sex (out of a total of 12 investigating the larval stage). As for tissue type, whole flies were studied 27 times, the thorax was used in 22 studies, while we could only find 2 studies on fly heads and 1 study on reproductive tissues (testes and ovaries). Mitochondrial preparations also varied, as pfi was used in 25 studies, thom in 20 and imt in 15 studies, respectively. MiR05 (the Oroboros-recommended respiration buffer) was the buffer of choice in 28 studies (including 1 using the MiR06 version), while 26 reports used one of two KCl-based buffers, and the remaining 6 used a sucrose-KCl buffer. Temperature in the O2k chambers was usually in the 24–25 °C range (45 studies), corresponding to the rearing temperature of the flies. However, 9 studies set the O2k chamber temperature at 37 °C without apparent justification (for example, assessing mitochondrial function at higher temperatures). Out of the 25 studies on pfi, 13 increased oxygen concentration in the O2k chambers prior to the SUIT protocols. Surprisingly, two

other studies increased oxygen levels, but using thom (Liu et al., 2020) and imt (Cruz et al., 2018), respectively. This raises the issue of hyperoxia, especially in imt, and puts the validity and comparability of the results into question. As the use of fluorescent probes to study ROS production is a relatively new addition to the Oroboros instrument, only 3 investigations reported their use simultaneously with O_2 flux analysis, all in 2021 and 2022. Finally, more than half (32/60) of the studies did not report *RCR* values, a marker of mitochondrial preparation quality. Among the remaining 28 studies, 5 did not explicitly state *RCR*s, however these could be estimated from the figures.

Table 1. Survey of studies using *Drosophila* species in the O2k-respirometer to assess mitochondrial bioenergetics, up to 01-06-2022, showing the wide variety of approaches and methods used in the field.

Ref.	*Drosophila spp.*, strain(s)	Sex	Tissue	Mt prep.	Resp. buffer	O2k temp.	+O_2 ?	ROS	*RCR*
Guitart 2010 J Biol Chem	*D. melanogaster*, UAS and GAL	Larvae unsexed	Whole larvae	pfi	MiR05	25 and 29 c	No	No	4 (est.)
Pichaud 2010 J Exp Biol	*D. simulans*	Males	Thorax	imt	KCl-1	12-28c range	No	No	5 to 8
Pichaud 2011 Am J Physiol Regul Integr Comp Physiol	*D. simulans*	Females	Thorax	pfi	KCl-1	12-28c range	No	No	4 to 8
Bratic 2011 PLOS Genetics	*D. melanogaster*, UAS-RNAi lines	Adults not specified and larvae unsexed	Thorax and whole larvae	pfi	Sucrose-KCl	25c	No	No	4 to 7
Stefanatos 2012 Cell Cycle	*D. melanogaster*, DAH and Ore	Adults, not specified	Whole fly	imt	KCl-1	25c	No	No	N.R.
Jumbo-Lucioni 2012 BMC Genomics	*D. melanogaster* inbred DGRP strains	Males and females	Thorax	imt	KCl-1	25c	No	No	10 (est.)
Correa 2012 Mitochondrion	*D. melanogaster*, Als, Dah, Jap, w1118	Males	Thorax	pfi	KCl-2:	25c	Yes	No	Above 13
Pimenta De Castro 2012 Cell Death Differ	*D. melanogaster*, transgenic strains	Males	Whole fly	thom	MiR05	37c	No	No	N.R.
Pichaud 2012 Evolution	*D. simulans*	Males	Thorax	pfi	KCl-1	24c	No	No	5
Costa 2013 Cell Death Dis	*D. melanogaster*, transgenic strains	Males	Whole fly	thom	MiR05	37c	No	No	6 (est.)
Wredenberg 2013 PLoS Genet	*D. melanogaster*, transgenic strains	Larvae unsexed	Whole larvae	pfi	Sucrose-KCl	25c	No	No	4 to 7
De Castro IP 2013 Cell Death Dis	*D. melanogaster*, transgenic strains	Adults, not specified	Whole fly	thom	MiR05	37c	No	No	N.R.

Macchi 2013 J Cell Sci	*D. melanogaster*, transgenic strains	Adults, not specified	Whole fly	thom	MiR05	37c	No	No	N.R.
Guitart 2013 Nucleic Acids Res	*D. melanogaster*, UAS and GAL	Larvae unsexed	Whole larvae	pfi	MiR05	25 and 29 c	No	No	4
Pichaud 2013 Mitochondrion	*D. melanogaster*, Jap and Als	Males	Thorax	pfi	KCl-2:	23c	Yes	No	Above 10
Baggio 2014 Nucleic Acids Res	*D. melanogaster*, UAS-RNAi lines	Males and females	Thorax and whole larvae	pfi	Sucros e-KCl	28c	No	No	N.R.
Tufi 2014 Nat Cell Biol	*D. melanogaster*, UAS-RNAi lines	Males	Whole fly and head	thom	MiR05	37c	No	No	N.R.
Kemppaine n 2014 Hum Mol Genet	*D. melanogaster*, transgenic strains	Larvae unsexed, adult males and females	Whole fly	thom	KCl-1	25c	No	No	N.R.
Bratic 2015 Nat Commun	*D. melanogaster*, RNAi lines	Larvae unsexed	Whole larvae	imt	MiR05	27c	No	No	N.R.
Rovenko 2015 Comp Biochem Physiol A Mol Integr Physiol	*D. melanogaster*, Canton S	Males and females	Whole fly	thom	KCl-1	25c	No	No	N.R.
Senyilmaz 2015 Nature	*D. melanogaster*, transgenic strains	Females	Whole larvae	pfi	MiR05	25c	Yes	No	4 (est.)
Syrjanen 2015 Front Zool	*D. melanogaster*, RNAi lines	Males and females	Whole fly	thom	KCl-1	25c	No	No	N.R.
Wolff 2016 J Evol Biol	*D. melanogaster*, mitonuclear strains	Males and females	Thorax	pfi	KCl-2:	25c	Yes	No	N.R.
Scialò 2016 Cell Metab	*D. melanogaster*, Dah transgenic	Females	Whole fly	thom	KCl-1	25c	No	No	N.R.
Scialò 2016 PLOS ONE	*D. melanogaster*, Dah transgenic	Females	Whole fly	thom	KCl-1	25c	No	No	N.R.
Bratic 2016 PLoS Genet	*D. melanogaster*, UAS-RNAi lines	Larvae unsexed	Whole larvae	pfi	Sucros e-KCl	25c	No	No	N.R.
Brandt 2017 eLife	*D. melanogaster*, Dah	Females	Whole fly	imt	Sucros e-KCl	37c	No	No	N.R.
De Carvalho 2017 Toxicol Research	*D. melanogaster*, Harwich strain	Males and females	Whole fly	imt	MiR05	24c	No	No	11 to 16
Lehmann 2017 Biology Open	*D. melanogaster*, various strains	Males	Whole fly	thom	MiR05	37c	No	No	N.R.
Rana 2017 Nat Commun	*D. melanogaster*, UAS-RNAi lines	Females	Head and thorax	pfi	MiR05	25c	Yes	No	N.R.
Ederer 2018 Int J Mol Sci	*D. melanogaster* inbred DGRP strains	Males	Whole fly	imt	KCl-1	25c	No	No	N.R.
Rodrigues 2018 Free	*D. melanogaster*, Ore	Females	Whole fly	imt	MiR05	24c	No	No	12

Radic Biol Med									
Cruz 2018 Chem Biol Interact	*D. melanogaster*, Harwich strain	Adults, not specified	Whole fly	Iit	KCl-1	25c	Yes	No	22
Rodrigues 2018 Sci Rep	*D. melanogaster*, UAS-RNAi lines	Larvae unsexed	Whole larvae	thom	KCl-1	25c	No	No	N.R.
Champigny 2018 Mar Drugs	*D. melanogaster*, w1118	Males	Thorax	pfi	KCl-1	24c	Yes	No	15 to 35
Thompson 2018 EMBO Mol Med	*D. melanogaster*, UAS-RNAi lines	Males	Whole fly	thom	KCl-1	25c	No	No	N.R.
Weisz 2018 Hum Mol Genet	*D. melanogaster*, various strains	Males	Thorax	imt	MiR05	25c	No	No	N.R.
Simard 2018 J Vis Exp	*D. melanogaster*, various strains	Males	Thorax	pfi	KCl-1	25c	Yes	No	6 to 33.55
Andreazza 2019 Nat Commun	*D. melanogaster*, various strains	Males	Whole fly	thom	Sucrose-KCl	30c	No	No	N.R.
Pajak 2019 PLoS Genet	*D. melanogaster*, UAS-RNAi lines	Larvae unsexed	Whole larvae	pfi	MiR05	25c	No	No	N.R.
Gururaja Rao 2019 Cells	*D. melanogaster*, various strains	Adults, not specified	Whole fly	imt	MiR05	25c	No	No	N.R.
Pichaud 2019 Front Genet	*D. melanogaster* Ore and Aut, D. simulans simw501	Females	Thorax	pfi	KCl-2:	24c	Yes	No	Above 10
Liu 2019 J Ethnopharmacol	*D. melanogaster*, PINK1 mutant	Males	Whole fly	thom	MiR05	37c	Yes	No	N.R.
Cormier 2019 Sci Rep	*D. melanogaster*, w1118	Males	Thorax	pfi	KCl-1	24c	Yes	No	10 to 20
Garrido-Maraver 2019	*D. melanogaster*, various strains	Males	Whole fly	thom	MiR05	37c	No	No	5 (est.)
Ulgherait 2020 Nat Commun	*D. melanogaster*, various strains	Males	Whole fly	imt	MiR05	25c	No	No	N.R.
Simard et al 2020 Metabolites	*D. melanogaster*, w1118	Males	Thorax	pfi	KCl-2:	24c	Yes	No	Above 10
Simard et al 2020b Metabolites	*D. melanogaster*, w1118	Males	Thorax	pfi	KCl-2:	24c	Yes	No	Above 10
Maddison 2020 PLoS Genet	*D. melanogaster*, various strains	Males	Whole fly	thom	MiR05	25c	No	No	N.R.
Kanellopoulos 2020 Cell	*D. melanogaster*, UAS and GAL	Males	Head and body	thom	MiR06	25c	No	No	N.R.
Cormier 2021 Insect Biochem Mol Biol	*D. melanogaster*, w1118	Males	Whole fly	imt	KCl-2:	24c	No	No	Above 10
Wall 2021 Dis Model Mech	*D. melanogaster*, transgenic strains	Males and females	Thorax	pfi	MiR05	25c	Yes	No	1 to 2

Jorgensen 2021 J Exp Biol	*Drosophila*, six different species	Females	Thorax	pfi	KCl-1	19-46c range	Yes	No	10
Rodriguez 2021 Front Genet	*D. melanogaster*, mitonuclear strains	Larvae unsexed	Whole larvae	pfi	MiR05	25c	No	Yes	6 to 15
Winwood-Smith 2021 Thesis	*D. melanogaster*, wild Australian strains	Females	Thorax	Imt	MiR05	25c	No	Yes	N.R.
Ebanks 2021 J Mol Sci	*D. melanogaster*, w1118	Males	Whole fly	thom	MiR05	20c	No	No	N.R.
Schober 2022 Hum Mol Genet	*D. melanogaster*, Dah transgenic	Larvae unsexed	Whole larvae	pfi	MiR05	25c	No	No	N.R.
Camus et al. Biorxiv 2022	*D. melanogaster*, mitonuclear strains	Males and females	Thorax and reproductive	pfi and thom	MiR05	25c	No	Yes	20 (thorax); 6 (testes and ovaries)
Ziech 2022 Drug Chem Tox	*D. melanogaster*, Harwich strain	Adults, not specified	Whole fly	imt	MiR05	24c	No	No	N.R.
Menail 2022 Front Phys	*D. melanogaster*, w1118	Males	Thorax	pfi	KCl-1	6-45c range	No	No	Above 10

Mitochondrial (mt) preparations: pfi = permeabilized fibers, thom = homogenates, imt = isolated mitochondria. Respiration buffer composition: MiR05 = 110 mM Sucrose, 60 mM Lactobionic acid, 20 mM Taurine, 20 mM HEPES, 10 mM KH_2PO_4, 3 mM $MgCl_2$, 0.5 mM EGTA, 1 % BSA, pH 7.1; MiR06 = MiR05 + Catalase; Sucrose-KCl = 120 mM Sucrose, 50 mM KCl, 20 mM Tris-HCl, 4 mM KH_2PO_4, 2 mM $MgCl_2$, 1 mM EGTA, pH 7.2; KCl-1 = 120 mM KCl, 5 mM KH_2PO_4, 3 mM HEPES, 1 mM EGTA, 1 mM $MgCl_2$, 0.2 % BSA, pH 7.2; KCl-2: 115 mM KCl, 10 mM KH_2PO_4, 2 mM $MgCl_2$, 3 mM HEPES, 1 mM EGTA, 0.2 % BSA, pH 7.2. *RCR*: est. = estimated from LEAK to OXPHOS respiration reported in graphical form in the paper; N.R. = not reported.

3.2. No evidence for oxygen diffusion limit in *Drosophila melanogaster* thorax tissue

The behaviour of the oxygen-dependent O_2 flux showed that it was indistinguishable from isolated mitochondria of the same tissue and species. This is illustrated in Figure 1 panels A-D, where the rapid decrease in the red O_2 flux trace happens suddenly and at low O_2 concentrations. This was observed in all treatments: hyperoxic (Figure 1A, B) and normoxic O_2 (Figure 1C) concentrations for thorax pfi in both sexes, as well as for imt (Figure 1D). Figure 2A shows O_2 flux normalised as flux control ratio (*FCR*, where maximum coupled respiration is set as = 1) as a function of O_2 concentration, in two representative normoxic and hyperoxic experiments (the same as Figure 1A and C). We observe a nearly identical behaviour of the two curves, showing almost no dependence of O_2 flux on O_2 concentration, until a very low level of O_2 is reached in the chamber. We then compared the apparent K_m for oxygen, or c_{50}, between normoxia and hyperoxia. For each experiment, we extracted the equation of the curve to obtain the c_{50} value for normoxic (n = 6) and hyperoxic conditions (n = 12) in males and females (details in Table S1). We found no impact of sex on the results; therefore, we combined the analysis of the results for males and females. Figure 2B shows the c_{50} values for pfi treated at normoxic (c_{50} = 0.38±0.07) and hyperoxic conditions (c_{50} = 0.82±0.08) in males and females. Although a two-sample t test showed a significant difference between the two treatments (p = 0.002), both values represent extremely low levels of oxygen in the chamber and are likely not biologically relevant (see Discussion).

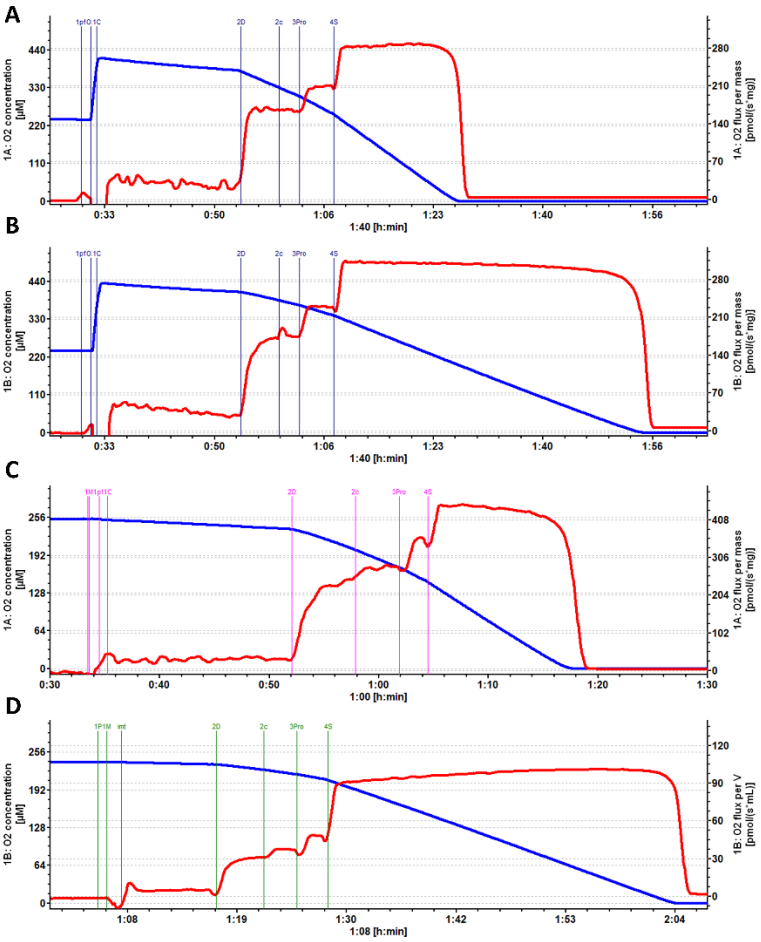

Figure 1. Representative oxygraph traces of *Drosophila* pfi respiration for female **(A)**, male **(B)** with addition of pure oxygen to the chamber (indicated by the increase in the blue oxygen concentration at the start of the experiment), and female with normal saturation of oxygen **(C)** versus isolated mitochondria (imt, **D)**. DatLab files of experiments "7-09-2021 P1-02 WT F vs M.DLD" (A and B), and "22-10-2021 P1-01 WT F pfi vs WT F Imt.DLD" (C and D).

3.3. Thorax homogenates are not a suitable alternative to permeabilized fibres

Thoracic tissue preparations thom and pfi differed markedly in various mitochondrial respiration parameters (Figure 3). O_2 flux was significantly reduced in tissue homogenates (thom) compared with permeabilized fibres (pfi) in WT flies. Compared to pfi, thom preparations had lower respiration rates in the N_P state: J_{O_2} (thom) = 58.22 (±8.57) $pmolO_2 \cdot s^{-1} \cdot mg^{-1}$, versus J_{O_2} (pfi) = 138.52 (±46.83) $pmolO_2 \cdot s^{-1} \cdot mg^{-1}$ (p = 0.002, Figure 3A). Coupling efficiency with N-linked substrates pyruvate and malate was also reduced in thom: $j \approx P_{thom}$ = 0.73 (±0.02), compared to $j \approx P_{pfi}$ = 0.88 (±0.03) (p = 0.008, Figure 3B); and the cytochrome *c* effect was higher in homogenates, indicating outer mitochondrial membrane damage: increase in J_{O_2} after cyt *c* addition was of 21 % (±6.42) in thom, compared to 0.51 % (±0.51) in pfi (p = 0.01, Figure 3C). Finally, H_2O_2 flux was 10 to 20-fold higher in thom than pfi for all respiratory states. In pfi, it ranged from 0.06 (±0.02) to 0.39 (±0.07) $pmolH_2O_2 \cdot s^{-1} \cdot mg^{-1}$ in N-linked coupled state (N_P) and maximum inhibition (ROX) respectively, while in thom it ranged from 0.97 (±0.05) to 3.85 (±0.34) $pmolH_2O_2 \cdot s^{-1} \cdot mg^{-1}$ in the two aforementioned states ($p \leq 0.01$, Figure 3D).

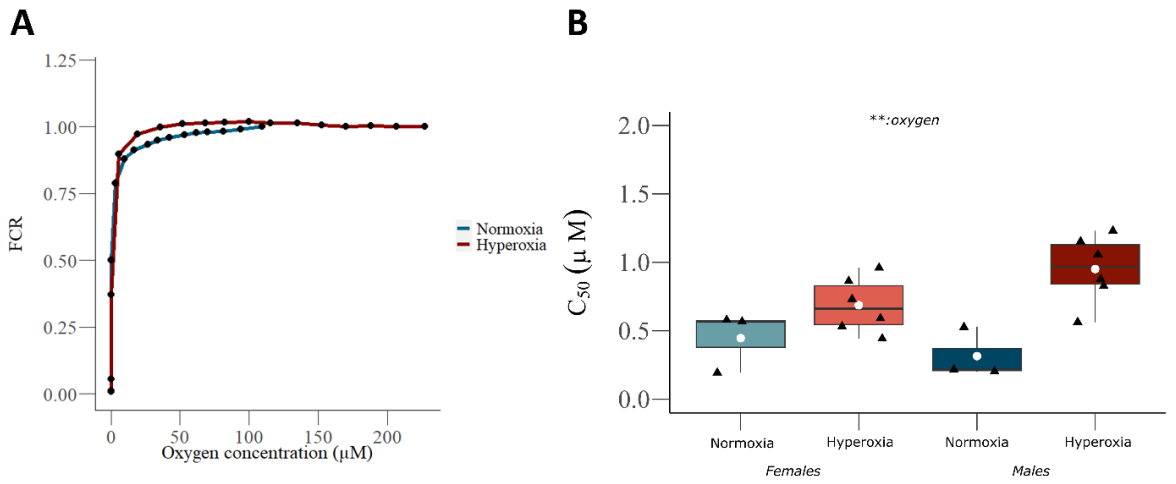

Figure 2. (A) O_2 flux presented as normalised flux control ratios (*FCR*) as a function of chamber O_2 concentration for pfi in normoxic and hyperoxic conditions (normal and high O_2). Curves are taken to two experiments: female normoxic (chamber A in "22-10-2021 P1-01 WT F pfi vs WT F Imt.DLD") and female hyperoxic (chamber A in "7-09-2021 P1-02 WT F vs M.DLD") and correspond to the traces shown in Figure 1C and 1A, respectively. **(B)** Calculated c_{50} of O_2 concentration-dependent O_2 flux for pfi in normoxic and hyperoxic conditions. Boxplots show median of runs (n=3 for each sex in normoxia, n=6 for each sex in hyperoxia), 25th and 75th percentiles, interquartile range and individual runs. Asterisks show a main effect of oxygen concentration (**$p \leq 0.01$; see Table S1).

3.4. Concentration-dependent effect of fluorescent probes

We compared the effect of titrating the fluorescent probes and their carrier solvent on N-linked respiration in the coupled state, after cytochrome *c* addition (Nc_P) and expressed as *FCR*s (Figure 4, Table S2). AmR exerted a significant (p = 0.05), effect at 12.5 and 15 µM when compared to the carrier solvent (DMSO), where a 18–20 % inhibition of O_2 flux was found: *FCR*=0.93 (±0.03) for DMSO versus 0.733 (±0.03) with AmR. MgG effect did not significantly differ from the effect of the carrier H_2O: at the highest concentration (1.65 µM), *FCR*=0.92 (±0.003) compared to 0.88 (±0.03) with MgG (p = 0.22). Rh123 exerted a significant effect on N-linked respiration compared to ethanol. Even at the mid-range concentration of 0.6 µM, it exerted a 13 % inhibition compared to ethanol: *FCR* = 0.94 (±0.02) compared to 0.81 (±0.01) with the probe (p = 0.007). The effect of Safranin was particularly strong after 1.5 µM. At the recommended final concentration of 2.0 µM, a 13 % inhibition was found, albeit not significant. Inhibition was of 30 % and significant (p = 0.006) at 2.5 µM: *FCR* = 0.97 (±0.03) with H_2O, compared to 0.67 (±0.02) with Saf. Finally, TMRM had a significant effect on respiration at every titration step, compared to DMSO: even at the second-lowest recommended concentration of 1 µM, it exerted a significant inhibition of 11 % (p = 0.04), *FCR* = 0.98 (±0.02) for DMSO versus 0.86 (±0.02) for TMRM. For the detailed results see Table S2.

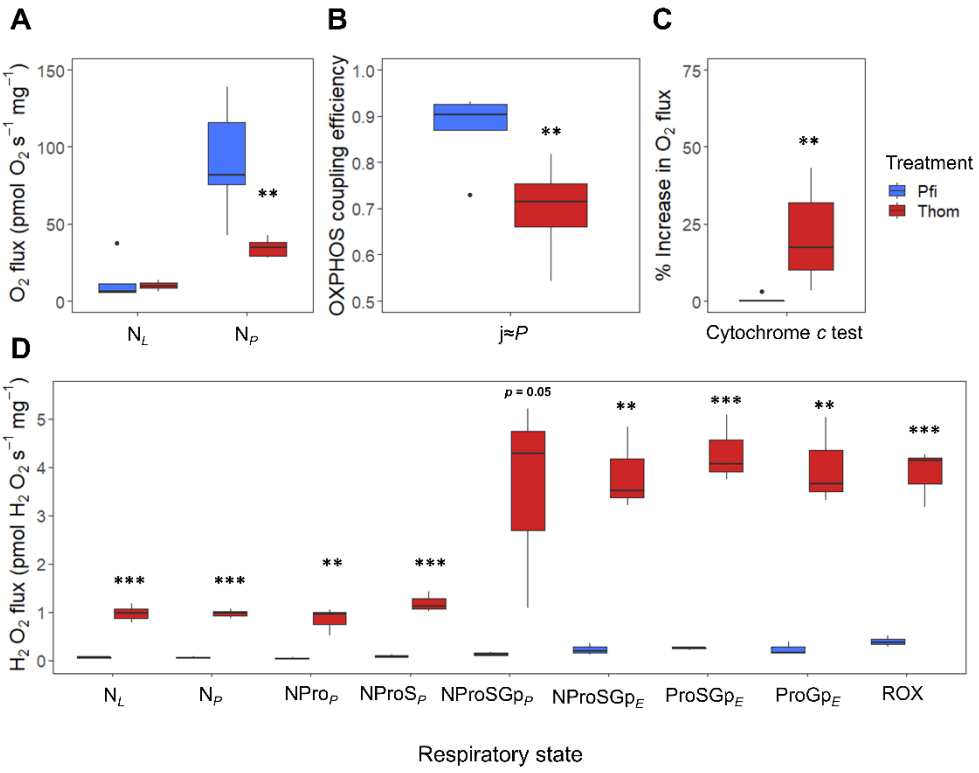

Figure 3. Fluorespirometry of permeabilized fibres (blue plots) versus tissue homogenates (red plots) in *D. melanogaster* thoraces. (A) LEAK and OXPHOS state: O_2 flux is normalised by mg wet tissue in the LEAK (N_L) and OXPHOS (N_P) states, fuelled with Complex I substrates (N-pathway). **(B)** OXPHOS coupling efficiency (j≈*P*) with N-pathway substrates **(C)** Mitochondrial membrane damage test through cytochrome *c* addition. **(D)** H_2O_2 flux in different respiratory states. Acronyms show substrates used: proline (Pro), succinate (S) and glycerophosphate (Gp); and states: ETS or maximum uncoupled respiration (*E*), residual oxygen consumption (ROX, after inhibition of Complexes I, II and III). Boxplots depict median values for each treatment (pfi or thom), 25th and 75th percentiles, interquartile range and outliers. Replicates per treatment: $n = 5$ for panels (A)-(B); $n = 6$ for panel (c); $n = 3$ for panel (D). Asterisks show significant differences (*$p \leq 0.05$, **$p \leq 0.01$, ***$p \leq 0.001$; two-sample *t* tests) between treatments.

4. Discussion

The variety of approaches to studying *Drosophila* mitochondrial function in the circa 60 studies surveyed over a 12-year period calls for a more careful consideration of the methodological approach tailored to the research questions. Investigators need to think about the suitability of their high-resolution respirometry approach, and not merely adopt previous protocols, where parameters such as chamber temperature might be unsuitable for their study model (e.g. in studies conducted at 37 °C in mammals, and at the same temperature in flies). The purpose of this report is to help investigators choose the best conditions for their mitochondrial function analyses, warning about potential

pitfalls and limitations. For example, adding extra oxygen to isolated mitochondria or homogenates can be problematic for interpreting results in light of ROS management (Munro and Treberg, 2017, Puma et al., 2020, Treberg, 2021), and might reflect how mitochondria from different fly lines or treatment react to hyperoxic conditions, rather than reflecting *in vivo* function. Moreover, analysing mitochondrial function at higher temperatures than the flies' rearing conditions might not test standard mitochondrial function, but rather heat resistance, and this might not be the question central to the study. Assessment of the quality of mitochondrial preparations is critical for all studies, and where cytochrome *c* tests cannot be done in every run (for example, if they interfere with fluorescence signals), *RCR* and/or *P-L* control efficiency (Gnaiger, 2020) values should be reported for the sake of transparency and comparison with previous studies. Finally, the male bias of *Drosophila* studies confirms what many researchers have been warning about – sex discrepancy in biomedical research. We therefore encourage investigators to study and compare both sexes where possible.

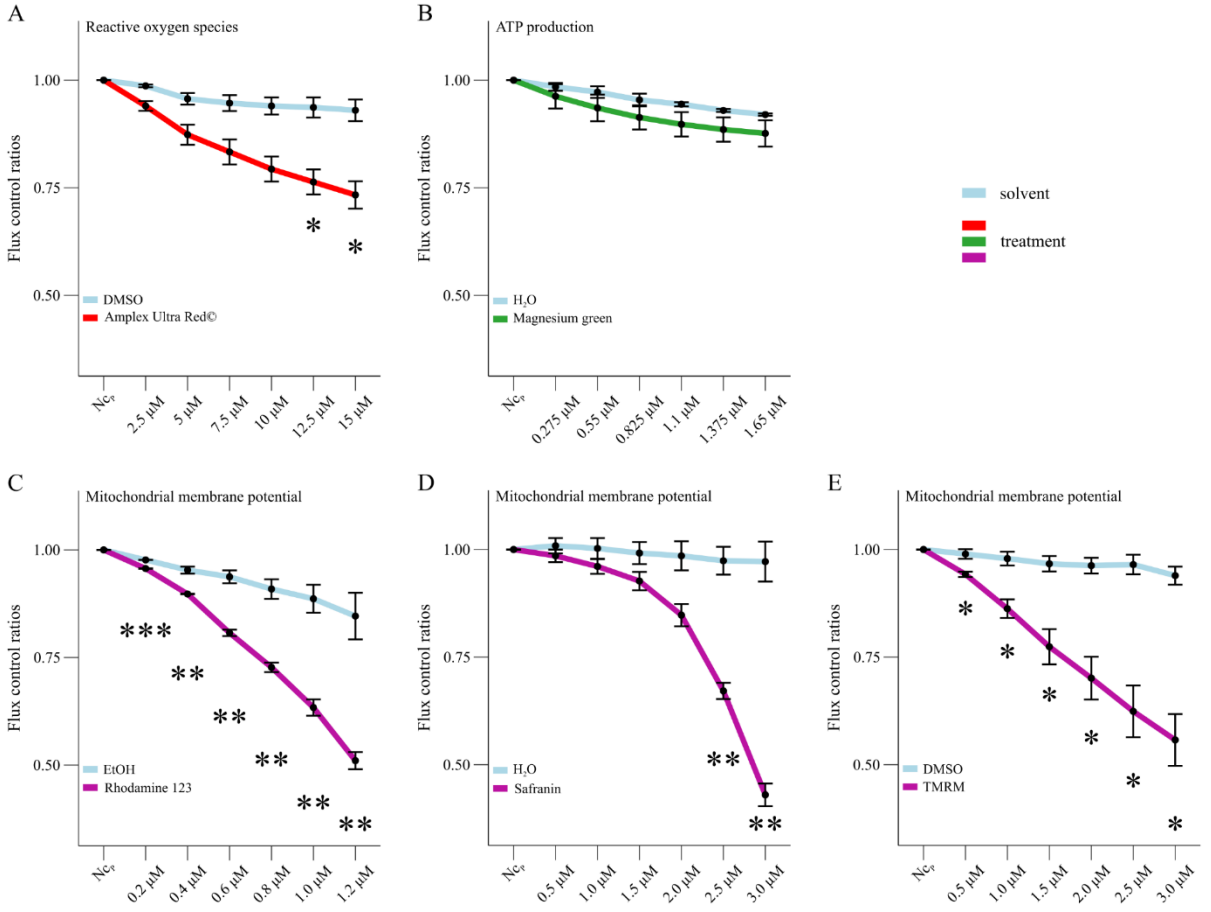

Figure 4. Effect of various fluorescent probes on N-pathway linked respiration in *Drosophila* thoraces pfi. (A) Amplex Ultra Red titration compared to the carrier DMSO. **(B)** Magnesium Green compared to water. **(C)** Rhodamine 123 compared to ethanol. **(D)** Safranin versus water. **(E)** TMRM compared to DMSO. Data are presented as means of n=6 experiments for each probe. The effect of probe presence was inferred at each titration point by means of a two-samples t test. p-values were adjusted using Holm's correction for multiple testing: *$p \leq 0.05$; **$p \leq 0.01$; ***$p \leq 0.001$.

We report a negligible oxygen dependence of respiration in permeabilized fibres from *Drosophila* thorax, with a 50 % decrease in respiration rate occurring at oxygen levels below 1 µM both in initial experimental normoxic or hyperoxic conditions, in females and males (Figure 2B, Table S1). Although we found a difference in the apparent K_m for oxygen (or c_{50} value) between hyperoxia and normoxia, both were between 50 and 100-fold lower than the 50 µM result reported by Pesta and Gnaiger (2012) for permeabilized fibres from human *v. lateralis* for ADP-stimulated respiration (with similar values for rat soleus and heart). A near-hyperbolic oxygen dependence of respiration was apparent in the mammalian study, while our results in flies showed no differences in the behaviour of the oxygen flux traces at low concentrations (Figure 1 and 2A) – almost indistinguishable from isolated mitochondria from *Drosophila* thorax. Hence, despite more than half of the studies on this tissue and species (Table 1), we conclude that it is not necessary to increase the amount of oxygen in the O2k-chamber before measuring mitochondrial respiration in *Drosophila* thorax pfi. In fact, it is likely that these hyperoxic conditions do not represent the physiological functioning of flight muscle in flies, and might impact ROS balance by increasing rates of production. We therefore recommend that future studies do not hyperoxygenate at the start of a SUIT protocol in thorax pfi, as respiration will remain stable at very low levels of oxygen. We suspect that this finding applies to the flight muscle of other flying insects, but researchers are encouraged to validate this by following the protocols outlined here.

A crucial step when measuring mitochondrial function is tissue preparation, as this will impact the quality and reproducibility of the data. An ideal tissue preparation must be as fast, reproducible and physiologically relevant as possible to address the questions studied. We report that the use of tissue homogenates of *Drosophila* thorax might not be appropriate with two types of homogenisers: the PBI-Shredder, and the handheld pellet pestle homogeniser. Both approaches yielded less coupled, more damaged mitochondria with lower rates of respiration, and much higher rates of H_2O_2 efflux (Figure 3). The use of *Drosophila* thom, with the two homogenisers tested in this study, is therefore not recommended. Other softer means of preparing thom might be considered; indeed, a soft dounce homogenizer, where a specific rotation speed can be chosen, reportedly yields good quality thom mitochondrial preparation (Dr. Brian Irving, *personal communication*). The PBI-Shredder has to our knowledge only been successfully used on mice and fish heart, brain and liver tissues (Doerrier et al., 2015, Eigentler et al., 2015). Therefore, researchers need to carefully consider their mt-preparation of choice, test and compare their values for O_2 flux, coupling, cytochrome *c* tests and H_2O_2 efflux with previously published results.

The development of fluorescent probes to study various mitochondrial parameters has multiplied over the last decades, with these applications reaching the O2k-FluoRespirometer environment more recently with the introduction of the Fluo-Sensors (Gnaiger et al., 2021). These applications are not yet widespread to the *Drosophila* mitochondrial field, therefore we sought to evaluate their applicability. We titrated some of the most commonly used fluorescent agents to test its concentration-dependent effect on respiration in *Drosophila* thorax (Figure 4, Table S2). While the ATP production probe Magnesium Green (MgG) exerted no significant effect on N-linked respiration (as previously reported by Cardoso et al., 2021), we found strong inhibitory effects of mitochondrial membrane potential probes Rhodamine 123 (Rh123), Safranin (Saf) and Tetramethyrhodamine methyl ester perchlorite (TMRM), as well as a moderate effect of the H_2O_2 detector Amplex Ultra Red (AmR). The concentrations recommended by the

manufacturer of the O2k-FluoRespirometer vary depending on the specific probe. At 10 µM AmR, the inhibition of around 15 % was not significantly distinguishable from the effect of the carrier (DMSO), and therefore appears acceptable for measurements. At the suggested range of 0.2–1 µM for Rh123, the inhibition was significantly higher than for the carrier (EtOH), and reached over 25 % N-pathway inhibition after 0.5 µM. Safranin strongly inhibited N-linked respiration at 2.5 µM, which was above the 2.0 µM suggested concentration (that showed a 15 % inhibition of respiration). TMRM is recommended to be used at 0.5–2 µM, and all these concentration steps significantly inhibited respiration compared to the carrier DMSO, although the lower range might be suitable and comparable to Safranin and AmR (around 15 % inhibitory effect). Therefore, we recommend careful consideration and fine-tuning of the concentration before use by researchers wanting to assess these parameters. For example, experiments can be run at the lower concentration end of quenching mode, but the intensity of fluorescence can be increased to be able to obtain a good signal to noise ratio. It appears difficult to avoid a certain degree of inhibition with the currently available probes on the market, but it is important for researchers to be aware of this and to work with concentrations that minimise these effects. More research needs to be done on the development of better reporter probes to assess all types of mitochondrial parameters.

Research in the biological and biomedical fields is currently facing a reproducibility crisis (Baker, 2016, Gnaiger, 2019). One way to address and attempt to solve this crisis involves being more thoughtful and transparent when choosing methodological approaches, and harmonising these techniques where possible. We hope that our study will give researchers a better overview of the "do's and don'ts" when it comes to assessing mitochondrial function in *Drosophila*.

Acknowledgements

We thank Rebecca Finlay for her help with fly husbandry.

References

Baker M. (2016) 1,500 scientists lift the lid on reproducibility. https://doi.org/10.1038/533452a

Camus MF, Clancy David J, Dowling Damian K. (2012) Mitochondria, Maternal Inheritance, and Male Aging. https://doi.org/10.1016/j.cub.2012.07.018

Camus MF, Kotiadis V, Carter H, Rodriguez E, Lane N. (2022) Mitonuclear interactions produce extreme differences in response to redox stress https://doi.org/10.1101/2022.02.10.479862

Cardoso LHD, Doerrier C, Gnaiger E. (2021) Magnesium Green for fluorometric measurement of ATP production does not interfere with mitochondrial respiration. https://doi.org/10.26124/bec:2021-0001

Carnegie L, Reuter M, Fowler K, Lane N, Camus MF. (2021) Mother's curse is pervasive across a large mitonuclear Drosophila panel. https://doi.org/10.1002/evl3.221

Cormier RPJ, Champigny CM, Simard CJ, St-Coeur P-D, Pichaud N. (2019) Dynamic mitochondrial responses to a high-fat diet in Drosophila melanogaster. https://doi.org/10.1038/s41598-018-36060-5

Correa CC, Aw WC, Melvin RG, Pichaud N, Ballard JWO. (2012) Mitochondrial DNA variants influence mitochondrial bioenergetics in Drosophila melanogaster. https://doi.org/10.1016/j.mito.2012.06.005

Cruz LC, Ecker A, Rodrigues NR, Martins IK, Posser T, Maciel FE, et al. (2018) Honey protects against wings posture error and molecular changes related to mitochondrial pathways induced by hypoxia/reoxygenation in adult Drosophila melanogaster. https://doi.org/10.1016/j.cbi.2018.06.033

Doerrier C, Draxl A, Wiethuechter A, Eigentler A, Gnaiger E. (2015) Mitochondrial respiration in permeabilized fibers versus homogenate from fish liver and heart. An application study with the PBI-Shredder. https://wiki.oroboros.at/index.php/MiPNet17.03_Shredder_vs_Fibers

Doerrier C, Garcia-Souza LF, Krumschnabel G, Wohlfarter Y, Mészáros AT, Gnaiger E (2018) High-Resolution FluoRespirometry and OXPHOS protocols for human cells, permeabilized fibers from small biopsies of muscle, and isolated mitochondria. https://doi.org/10.1007/978-1-4939-7831-1_3

Eigentler A, Draxl A, Fontana-Ayoub M, Gnaiger E. (2015) Tissue homogenates for diagnosis of mitochondrial respiratory function: Mouse heart, brain and liver. https://wiki.oroboros.at/index.php/MiPNet17.15_PBI-Shredder_Mouse-heart-brain-liver

Gnaiger E. (2019) Editorial: A vision on preprints for mitochondrial physiology and bioenergetics. https://doi.org/10.26124/mitofit:190002.v2

Gnaiger E. (2020) Mitochondrial pathways and respiratory control. An introduction to OXPHOS analysis. 5th ed. https://doi.org/10.26124/bec:2020-0002

Gnaiger E - MitoEAGLE Task Group (2020) Mitochondrial physiology. https://doi.org/10.26124/bec:2020-0001.v1

Gnaiger E, Komlódi T, Schmitt S, Cecatto C, Gradl L, Gradl P. (2021) O2k-FluoRespirometer manual. https://wiki.oroboros.at/index.php/MiPNet22.11_O2k-FluoRespirometer_manual

Jørgensen LB, Overgaard J, Hunter-Manseau F, Pichaud N. (2021) Dramatic changes in mitochondrial substrate use at critically high temperatures: a comparative study using Drosophila. https://doi.org/10.1242/jeb.240960

Kuznetsov AV, Veksler V, Gellerich FN, Saks V, Margreiter R, Kunz WS. (2008) Analysis of mitochondrial function in situ in permeabilized muscle fibers, tissues and cells. https://doi.org/10.1038/nprot.2008.61

Liu M, Yu S, Wang J, Qiao J, Liu Y, Wang S, et al. (2020) Ginseng protein protects against mitochondrial dysfunction and neurodegeneration by inducing mitochondrial unfolded protein response in Drosophila melanogaster PINK1 model of Parkinson's disease. https://doi.org/10.1016/j.jep.2019.112213

Markow TA. (2015) The secret lives of Drosophila flies. https://doi.org/10.7554/elife.06793

Morrow EH. (2015) The evolution of sex differences in disease. https://doi.org/10.1186/s13293-015-0023-0

Munro D, Treberg JR. (2017) A radical shift in perspective: mitochondria as regulators of reactive oxygen species. https://doi.org/10.1242/jeb.132142

Oroboros-Ecosystem. Permeabilized muscle fibers. 2016; Available from: https://wiki.oroboros.at/index.php/Permeabilized_muscle_fibers.

Oroboros-Ecosystem. O2k-Publications: Drosophila. 2023; Available from: https://wiki.oroboros.at/index.php/O2k-Publications:_Drosophila.

Pecinová A, Drahota Z, Nůsková H, Pecina P, Houštěk J. (2011) Evaluation of basic mitochondrial functions using rat tissue homogenates. https://doi.org/10.1016/j.mito.2011.05.006

Pesta D, Gnaiger E. (2012) High-resolution respirometry: OXPHOS protocols for human cells and permeabilized fibers from small biopsies of human muscle. https://doi.org/10.1007/978-1-61779-382-0_3

Pesta D, Gnaiger E. (2015) Preparation of permeabilized muscle fibers for diagnosis of mitochondrial respiratory function. https://wiki.oroboros.at/index.php/MiPNet14.14_PermeabilizedFiberPreparation

Pichaud N, Ballard JWO, Tanguay RM, Blier PU. (2012) Naturally occurring mitochondrial dna haplotypes exhibit metabolic differences: Insight into functional properties of mitochondria. https://doi.org/ 10.1111/j.1558-5646.2012.01683.x

Pichaud N, Ballard JWO, Tanguay RM, Blier PU. (2011) Thermal sensitivity of mitochondrial functions in permeabilized muscle fibers from two populations of Drosophila simulans with divergent mitotypes. https://doi.org/10.1152/ajpregu.00542.2010

Pichaud N, Chatelain EH, Ballard JWO, Tanguay R, Morrow G, Blier PU. (2010) Thermal sensitivity of mitochondrial metabolism in two distinct mitotypes of Drosophila simulans: evaluation of mitochondrial plasticity. https://doi.org/10.1242/jeb.040261

Puma LCL, Hedges M, Heckman JM, Mathias AB, Engstrom MR, Brown AB, et al. (2020) Experimental oxygen concentration influences rates of mitochondrial hydrogen peroxide release from cardiac and skeletal muscle preparations. https://doi.org/10.1152/ajpregu.00227.2019

Quéméneur J-B, Danion M, Cabon J, Collet S, Zambonino-Infante J-L, Salin K. (2022) The relationships between growth rate and mitochondrial metabolism varies over time. https://doi.org/10.1038/s41598-022-20428-9

Rodríguez E, Grover Thomas F, Camus MF, Lane N. (2021) Mitonuclear Interactions Produce Diverging Responses to Mild Stress in Drosophila Larvae. https://doi.org/10.3389/fgene.2021.734255

Simard CJ, Pelletier G, Boudreau LH, Hebert-Chatelain E, Pichaud N. (2018) Measurement of Mitochondrial Oxygen Consumption in Permeabilized Fibers of Drosophila Using Minimal Amounts of Tissue. https://doi.org/gna10.3791/57376

Suarez RK. (2000) Energy Metabolism during Insect Flight: Biochemical Design and Physiological Performance. https://doi.org/10.1086/318112

Suarez RK. (1998) Oxygen and the upper limits to animal design and performance. https://doi.org/10.1242/jeb.201.8.1065

Thoral E, Roussel D, Chinopoulos C, Teulier L, Salin K. (2021) Low oxygen levels can help to prevent the detrimental effect of acute warming on mitochondrial efficiency in fish. https://doi.org/10.1098/rsbl.2020.0759

Treberg JR. (2021) Review: Using isolated mitochondria to investigate mitochondrial hydrogen peroxide metabolism. https://doi.org/10.1016/j.cbpb.2021.110614

Ventura-Clapier R, Moulin M, Piquereau J, Lemaire C, Mericskay M, Veksler V, et al. (2017) Mitochondria: a central target for sex differences in pathologies. https://doi.org/10.1042/cs20160485

Wolff JN, Pichaud N, Camus MF, Côté G, Blier PU, Dowling DK. (2016) Evolutionary implications of mitochondrial genetic variation: Mitochondrial genetic effects on OXPHOS respiration and mitochondrial quantity change with age and sex in fruit flies. https://doi.org/10.1111/jeb.12822

Zucker I, Beery AK. (2010) Males still dominate animal studies. https://doi.org/10.1038/465690a

Supplement

Table S1. Effect of sex and starting oxygen saturation level over the O_2 concentration at half respiration flux (C_{50}) in permeabilized *Drosophila melanogaster* thoraces.

ID	sex	oxygen	C_{50} (µM)
1Mh	M	hyperoxia	1.057
1Fh	F	hyperoxia	0.962
2Fh	F	hyperoxia	0.863
3Fh	F	hyperoxia	0.532
2Mh	M	hyperoxia	1.231
3Mh	M	hyperoxia	1.153
4Fh	F	hyperoxia	0.590
4Mh	M	hyperoxia	0.828
5Fh	F	hyperoxia	0.733
5Mh	M	hyperoxia	0.878
6Fh	F	hyperoxia	0.445
6Mh	M	hyperoxia	0.563
1Fn	F	normoxia	0.580
1Mn	M	normoxia	0.528
2Fn	F	normoxia	0.194
2Mn	M	normoxia	0.203
3Fn	F	normoxia	0.566
3Mn	M	normoxia	0.215

LM var~sex*oxygen	*mean ± s.e.m*	F-normoxia	0.447 ± 0.126
		F-hyperoxia	0.687 ± 0.082
		M-normoxia	0.316 ± 0.106
		M-hyperoxia	0.952 ± 0.1
	:sex		*F*=1.4417, *P*=0.2484
	:oxygen		***F*=14.02, *P*=0.0019** **
	:sex:oxygen		/

Respirometry data were normalized for the maximal coupled respiration and expressed as flux control ratios (FCR). Factors: *'oxygen'*: hyperoxia (n=12), normoxia (n=6); *'sex'*: females (F, n=9) and males (M, n=9). The main effects of factors sex and oxygen saturation level and their interaction were inferred by means of a linear model followed by anova test. The best fitting model was determined though sequential model simplification. Dashed out cells are the result of step-wise model simplification. *:sex,* main effect of sex; *:oxygen*, main effect of oxygen concentration; *:sex:oxygen*, interaction. *$p \leq 0.05$; **$p \leq 0.01$; ***$p \leq 0.001$. Data are presented separately and also as mean ± standard error of the mean (sem). Data refer to Figure 2B

Table S2. Impact of fluorescent probes on mitochondrial respiration in permeabilized Drosophila melanogaster thoraces. Respirometry data were normalized for a common internal parameter, the CI-sustained coupled respiration in absence of fluorescent probes ('NcP'), and expressed as flux control ratios (FCR).

probe	treatment	N_{CP}	titration 1	titration 2	titration 3	titration 4	titration 5	titration 6
AmR	ctrl	1	0.9900	0.9700	0.9700	0.9600	0.9600	0.9500
AmR	treatment	1	0.9400	0.8800	0.8400	0.8000	0.7700	0.7300
AmR	ctrl	1	0.9900	0.9700	0.9600	0.9600	0.9600	0.9600
AmR	treatment	1	0.9600	0.9100	0.8800	0.8400	0.8100	0.7900
AmR	ctrl	1	0.9800	0.9300	0.9100	0.9000	0.8900	0.8800
AmR	treatment	1	0.9200	0.8300	0.7800	0.7400	0.7100	0.6800
AmR	ctrl (mean ± sem)	1 ± 0	0.987 ± 0.003	0.957 ± 0.013	0.947 ± 0.019	0.94 ± 0.02	0.937 ± 0.023	0.93 ± 0.025
	treatment (mean ± sem)	1 ± 0	0.94 ± 0.012	0.873 ± 0.023	0.833 ± 0.029	0.793 ± 0.029	0.763 ± 0.029	0.733 ± 0.032
	t=3.8829, *P*=0.0178*			*t*=3.1009, *P*=0.03619*	*t*=3.2869, *P*=0.0303*	*t*=4.1576, *P*=0.01417*	*t*=4.651, *P*=0.009654**	*t*=4.8498, *P*=0.008341**
	p adjusted		0.0567·	0.0606·	0.0606·	0.0567·	0.0500*	0.0500*
MgG	ctrl	1	0.9963	0.9983	0.982	0.9534	0.9363	0.925
MgG	treatment	1	0.9808	0.9721	0.9426	0.913	0.899	0.8986
MgG	ctrl	1	0.9663	0.9529	0.9319	0.94	0.9265	0.9194
MgG	treatment	1	0.9068	0.8742	0.8574	0.8423	0.8306	0.8161
MgG	ctrl	1	0.9909	0.9658	0.9484	0.9386	0.9263	0.9159
MgG	treatment	1	1	0.9601	0.9402	0.9371	0.9264	0.9141
MgG	ctrl (mean ± sem)	1 ± 0	0.984 ± 0.009	0.972 ± 0.014	0.954 ± 0.015	0.944 ± 0.005	0.93 ± 0.003	0.92 ± 0.003
	treatment (mean ± sem)	1 ± 0	0.963 ± 0.028	0.935 ± 0.031	0.913 ± 0.028	0.897 ± 0.028	0.885 ± 0.028	0.876 ± 0.03
	t=0.73529, *P*=0.5029			*t*=1.0953, *P*=0.3349	*t*=1.2859, *P*=0.2679	*t*=1.6137, *P*=0.1819	*t*=1.5471, *P*=0.1967	*t*=1.4358, *P*=0.2244
	p adjusted		1	1	1	1	1	1
Rh123	ctrl	1	0.9769	0.9623	0.9516	0.9498	0.9431	0.9383
Rh123	treatment	1	0.9558	0.8966	0.8146	0.7216	0.6111	0.4878
Rh123	ctrl	1	0.9768	0.9602	0.9531	0.9066	0.8864	0.8492
Rh123	treatment	1	0.9582	0.8992	0.7922	0.7112	0.6186	0.493
Rh123	ctrl	1	0.9763	0.9369	0.9075	0.8709	0.8298	0.7509
Rh123	treatment	1	0.9559	0.8968	0.8148	0.7484	0.6714	0.5502
Rh123	ctrl (mean ± sem)	1 ± 0	0.977 ± 0	0.953 ± 0.008	0.937 ± 0.015	0.909 ± 0.023	0.886 ± 0.033	0.846 ± 0.054
	treatment (mean ± sem)	1 ± 0	0.957 ± 0.001	0.898 ± 0.001	0.807 ± 0.008	0.727 ± 0.011	0.634 ± 0.019	0.51 ± 0.02
	t=6.9479, *P*=3.957e-05***			*t*=6.7954, *P*=0.002449**	*t*=7.7817, *P*=0.001471**	*t*=7.178, *P*=0.001995**	*t*=6.6839, *P*=0.002605**	*t*=5.8204, *P*=0.004339**
	p adjusted		0.00023742***	0.00798**	0.00735**	0.00798**	0.00798**	0.00798**
Saf	ctrl	1	0.998	0.991	0.9882	0.982	0.9758	0.9741
Saf	treatment	1	0.9748	0.9472	0.9144	0.8444	0.6538	0.3893
Saf	ctrl	1	0.9849	0.9684	0.9493	0.9286	0.917	0.8904
Saf	treatment	1	1.0143	0.9946	0.9684	0.8939	0.7093	0.4789
Saf	ctrl	1	1.0434	1.0485	1.0377	1.0455	1.0289	1.0512
Saf	treatment	1	0.9668	0.9402	0.8975	0.8045	0.6518	0.4219
Saf	ctrl (mean ± sem)	1 ± 0	1.009 ± 0.018	1.003 ± 0.024	0.992 ± 0.026	0.985 ± 0.034	0.974 ± 0.032	0.972 ± 0.046
	treatment (mean ± sem)	1 ± 0	0.985 ± 0.015	0.961 ± 0.017	0.927 ± 0.021	0.848 ± 0.026	0.672 ± 0.019	0.43 ± 0.026
	t=1.0196, *P*=0.3656			*t*=1.4307, *P*=0.2258	*t*=1.9487, *P*=0.1231	*t*=3.238, *P*=0.03173*	*t*=8.0802, *P*=0.001275**	*t*=10.165, *P*=0.000527***
	p adjusted		0.4516	0.4516	0.3693	0.12692	0.006375**	0.003164**
TMRM	ctrl	1	1.0026	0.9952	0.9815	0.985	1.0065	0.9773
TMRM	treatment	1	0.9513	0.8678	0.7645	0.6772	0.5793	0.5116
TMRM	ctrl	1	0.9676	0.9467	0.9315	0.927	0.9277	0.905
TMRM	treatment	1	0.9455	0.8971	0.8492	0.7967	0.7429	0.6765
TMRM	ctrl	1	0.9984	0.9951	0.9877	0.9759	0.9609	0.936
TMRM	treatment	1	0.9305	0.8225	0.7088	0.6296	0.5499	0.4846
TMRM	ctrl (mean ± sem)	1 ± 0	0.99 ± 0.011	0.979 ± 0.016	0.967 ± 0.018	0.963 ± 0.018	0.965 ± 0.023	0.939 ± 0.021
	treatment (mean ± sem)	1 ± 0	0.942 ± 0.006	0.862 ± 0.022	0.774 ± 0.041	0.701 ± 0.05	0.624 ± 0.06	0.538 ± 0.06
	t=3.7219, *P*=0.02044*			*t*=4.3081, *P*=0.01257*	*t*=4.3286, *P*=0.01236*	*t*=4.9458, *P*=0.00784**	*t*=5.3087, *P*=0.006052**	*t*=6.0112, *P*=0.003856**
	p adjusted		0.03708*	0.03708*	0.03708*	0.031136*	0.03026*	0.023136*

Probes: 'AmR': Amplex® UltraRed (n = 3; solvent: DMSO); 'MgG': Magnesium green (n = 3; solvent: H_2O); 'Rh123': Rhodamine 123 (n = 3; solvent: EtOH); 'Saf': Safranin O (n = 3; solvent: H_2O); 'TMRM': Tetramethylrhodamine methyl ester (n = 3; solvent: DMSO). Each probe was tested at different sequential concentrations: AmR ('2.5 µM', '5 µM', '7.5 µM', '10 µM', '12.5 µM' and '15 µM'); MgG: ('0.275 µM', '0.55 µM', '0.825 µM', '1.1 µM', '1.375 µM' and '1.65 µM'); Rh123: ('0.2 µM', '0.4 µM', '0.6 µM', '0.8 µM', '1.0 µM' and '1.2 µM'); Saf: ('0.5 µM', '1.0 µM', '1.5 µM', '2.0 µM', '2.5 µM' and '3.0 µM'); TMRM: ('0.5 µM', '1.0 µM', '1.5 µM', '2.0 µM', '2.5 µM' and '3.0 µM'). Parallel controls were titrated with an equal volume of each probe-specific solvent. Factor: 'treatment' ('ctrl' = control using the specific solvent, 'treatment' = probe treatment). 'Nc_P': CI-sustained coupled respiration of permebilized tissue. The effect of probe presence (':treatment') was inferred at each titration point by means of a two samples t test. p-values were adjusted using Holm's correction for multiple testing. ·0.05 > p ≤ 0.09; *p ≤ 0.05; **p ≤ 0.01; ***p ≤ 0.001. Data are presented separately and also as mean ± standard error of the mean (sem). Data refer to Figure 4.